Whole mount histological registration and validation of hierarchical clustering for segmentation of tumor and normal prostate using multi-parametric MRI

D. L. Langer[1,2], T. H. van der Kwast[3], A. J. Evans[3], S. Okhai[4], J. Trachtenberg[5], and M. A. Haider[1]

[1]Medical Imaging, University Health Network, Toronto, Ontario, Canada, [2]Institute of Medical Sciences, University of Toronto, Toronto, Ontario, Canada, [3]Pathology, University Health Network, Toronto, Ontario, Canada, [4]Sunnybrook Health Sciences Centre, Toronto, Ontario, Canada, [5]University Health Network, Toronto, Ontario, Canada

Introduction

Prostate cancer (PCa) localization is becoming of increasing importance with the use of targeted therapies. The full extent of a tumor within the prostate cannot be accurately characterized using T2 imaging alone, however there has been some success using multi-parametric analysis to map regions of tumor [1,2]. Accurate radiologic-pathologic correlation can be difficult due to variations in imaging planes and tissue geometry. To explore correspondence between imaging results and pathologic findings, we perform both *in vivo* and *ex vivo* MRI to match sections, then systematically register pathology to imaging results using a 5mm grid.

Purpose

To use hierarchical clustering to demonstrate that accuracy of tumor segmentation is increased with the use of a greater number of MRI parameters.

Materials and Methods

Five patients with known PCa underwent endorectal MRI on a 1.5T GE Excite HD platform prior to prostatectomy in this prospective study. Ethics board approval and informed consent was obtained. T2-weighted fast spin-echo (T2w), T2-mapping (T2) (TR: 2000ms, 10 TEs: from 9.4-94ms, matrix: 256x128, FOV: 20cm), DWI (TR/TE: 4000/77ms, matrix: 128x256, FOV: 14cm, b: 0, 600), and DCE (TR/TE: 4.3/1.9ms, matrix: 256x128, FOV: 20cm, α: 20°, temporal resolution: 10s) was performed. Slice thickness for all scans was 3mm. A Brix model [3] was used to calculate the rate constants k_{ep}, k_{el}, and parameter A by minimizing the sum of squared error (sse). Post-surgery, the excised prostate was fixed in formalin for 24 hours and embedded in HistOmer gel (Vibratome, St. Louis, MO) for *ex vivo* imaging and subsequent sectioning. Fast spin-echo (FSE) images were taken at 5° intervals to determine the angle corresponding to the plane of *in vivo* imaging. Once the angle was ascertained, a high resolution 3D fast recovery FSE dataset was acquired to register the pathology slices with imaging. Using a rotary blade, the gel-embedded sample was cut in 3mm sections along the same angled plane. The peripheral zone (PZ) was outlined on the T2w image, and the contour transferred to the other MRI datasets. Only voxels within the PZ were included in subsequent analysis. A 5mm grid was overlaid on all imaging and pathology specimens. Regions of tumor were outlined on the histological section by a pathologist, and each element was scored from -1 to 4 based on the percentage area occupied by tumor (outside of tissue: -1, normal tissue: 0, <25% tumor: 1, 25-50% tumor: 2, 50-75%: 3, >75%: 4). The median value of all voxels contained within a grid element was calculated, and was included in the analysis if more than 50% of the grid element contained voxels within PZ.

Nine whole mount sections were analyzed, two each from four patients and one from a fifth. Of the resulting 134 grid elements, 80 were scored as normal (score = 0), and 17 at a score of 4. To avoid partial volume effects, elements with pathology scores other than 0 and 4 were excluded. Feature vectors were constructed using 8 parameters (T2w, T2, ADC, FA, k_{ep}, k_{el}, A, sse), each normalized by the median value from the patient's normal tissue. Hierarchical clustering was performed using average linkage clustering, with the Pearson correlation as the distance metric. Three clusters, representing two normal tissue populations and one with a higher risk of disease, were determined. Sensitivity and specificity results were compared between the 8-parameter model, models including a subset of parameters for each MRI modality, and a 3-parameter model using T2w, ADC and k_{ep}.

Results and Discussion

Typical radiologic-pathologic correlation is shown in Figure 1. The 8-parameter model had the highest sensitivity and specificity for detecting cancer, as shown in Table 1. DCE parameters contribute the most to these results, and ADC the least, however sensitivity is reduced if ADC and FA are removed from the feature vector. The use of parameters from different MRI techniques in a vector increases sensitivity compared to using parameters from one dataset, as seen when T2w, ADC and k_{ep} are combined. Increasing the number of clusters may differentiate between high- and moderate-risk regions. With four clusters, the high-risk group in the 8-parameter model subdivides into two; one group containing 59% of all cancer elements, the other with 29%. This information could be used in target planning; however, pathologic validation of sub-populations must still be determined. To refine this study, we are pursuing the use of deformable registration and increasing our cohort of patients.

Conclusion

We have developed a technique to create whole mount sections from the same plane as *in vivo* MRI. Using hierarchical clustering, an 8-parameter model was able to better distinguish between normal and malignant tissues, compared to models using a subset of these. We demonstrate that using a larger number of features from multiple MRI datasets improves tumor segmentation. This methodology can be used to facilitate accurate mapping of MRI parameters to the pathologic prostate.

References: [1] Mazaheri *et al*, Proc Intl Soc Mag Reson Med 2006; 14:3497. [2] Carano *et al*, Magn Reson Med 2004; 51:542-551. [3] Tofts. JMRI 1997; 7:91-101

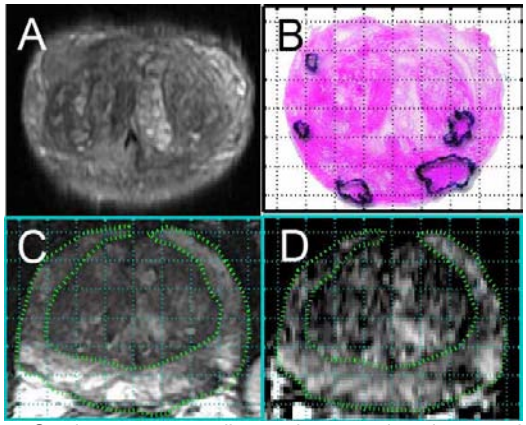

Figure 1. Sections corresponding to the same location are shown for *ex vivo* MRI (**A**), pathology (**B**), and *in vivo* T2w (**C**) and ADC (**D**). The 5mm grid is shown overlaid on **B-D** and the location of the grid can be seen to agree well. Regions of tumor are outlined in black in **B**, and the peripheral zone is defined using the green dotted line in **C** and **D**.

Table 1. Sensitivity and Specificity

Parameters in feature vector	Sensitivity	Specificity
T2w, T2	64.7	57.0
ADC, FA	47.1	57.0
k_{ep}, k_{el}, A, sse	76.5	67.1
T2w, ADC, k_{ep}	82.4	64.5
T2w, T2, k_{ep}, k_{el}, A, sse	82.4	70.9
8-parameter model:		
T2w, T2, ADC, FA, k_{ep}, k_{el}, A, sse	88.2	69.6